BJP British Journal of Pharmacology

DOI:10.1111/bph.13037
www.brjpharmacol.org

RESEARCH PAPER

# High-affinity σ1 protein agonist reduces clinical and pathological signs of experimental autoimmune encephalomyelitis

B Oxombre[1,2], C Lee-Chang[1,2,*], A Duhamel[1,3], M Toussaint[1,4], M Giroux[1,2,5], M Donnier-Maréchal[1,6], P Carato[1,6], D Lefranc[1,2], H Zéphir[1,2,5], L Prin[1,2,7], P Melnyk[1,4,6,8] and P Vermersch[1,2,5]

[1]*Université de Lille, Lille, France,* [2]*UDSL, EA2686-LIRIC, UFR Médecine, Lille, France,* [3]*UDSL, EA 2694, UFR Médecine, Lille, France,* [4]*CNRS UMR8161, Lille, France,* [5]*Centre Hospitalier Régional et Universitaire de Lille, Pôle de neurologie–Service de Neurologie D, Lille, France,* [6]*UDSL, EA 4481, UFR Pharmacie, Lille, France,* [7]*Centre Hospitalier Régional et Universitaire de Lille, Pôle d'immunologie–Centre de Biologie Pathologie et Génétique, Lille, France, and* [8]*Inserm UMR-S1172, Jean-Pierre Aubert Research Center, Lille, France*

**Correspondence**
Bénédicte Oxombre, 1 place de Verdun, 59045 Lille Cedex, France. E-mail: benedicte.vanteghem@univ-lille2.fr

*Present address: Laboratory of Molecular Biology and Immunology, National Institute on Aging, National Institutes of Health, Baltimore, MD, USA.

**Received**
11 March 2014
**Revised**
16 October 2014
**Accepted**
16 November 2014

## BACKGROUND AND PURPOSE

Selective agonists of the sigma-1 receptor (σ1 protein) are generally reported to protect against neuronal damage and modulate oligodendrocyte differentiation. Human and rodent lymphocytes possess saturable, high-affinity binding sites for compounds binding to the σ1 protein and potential immunomodulatory properties have been described for σ1 protein ligands. Experimental autoimmune encephalomyelitis (EAE) is recognized as a valuable model of the inflammatory aspects of multiple sclerosis (MS). Here, we have assessed the role of a σ1 protein agonist, containing the tetrahydroisoquinoline-hydantoin structure, in EAE.

## EXPERIMENTAL APPROACH

EAE was induced in SJL/J female mice by active immunization with myelin proteolipid protein $(PLP)_{139–151}$ peptide. The σ1 protein agonist was injected i.p. at the time of immunization (day 0). Disease severity was assessed clinically and by histopathological evaluation of the CNS. Phenotyping of B-cell subsets and regulatory T-cells were performed by flow cytometry in spleen and cervical lymph nodes.

## KEY RESULTS

Prophylactic treatment of EAE mice with the σ1 protein agonist prevented mononuclear cell accumulation and demyelination in brain and spinal cord and increased T2 B-cells and regulatory T-cells, resulting in an overall reduction in the clinical progression of EAE.

## CONCLUSIONS AND IMPLICATIONS

This σ1 protein agonist, containing the tetrahydroisoquinoline-hydantoin structure, decreased the magnitude of inflammation in EAE. This effect was associated with increased proportions of B-cell subsets and regulatory T-cells with potential immunoregulatory functions. Targeting of the σ1 protein might thus provide new therapeutic opportunities in MS.

## Abbreviations

Bregs, regulatory B cells; CFA, complete Freund's adjuvant; CLNs, cervical lymph nodes; EAE, experimental autoimmune encephalomyelitis; H&E, haematoxylin and eosin; LFB, luxol fast blue; MS, multiple sclerosis; MZ, marginal zone; PLP, myelin proteolipid protein; T2, transitional 2; Tregs, regulatory T cells

## Tables of Links

| TARGETS | |
|---|---|
| Sigma receptor, σ1 protein[a] | **Ligand-gated ion channels**[d] |
| **GPCRs**[b] | $IP_3$ receptors |
| Dopamine $D_1$ receptors | $GABA_A$ ionotropic receptors |
| Muscarinic receptors | Glutamate ionotropic receptors |
| **Catalytic receptor**[c] | Nicotinic receptors |
| TrkB, neurotrophic tyrosine kinase receptor type 2 | |

| LIGANDS |
|---|
| BD-1047 |
| IFN-γ |
| IL-17a |
| IL-4 |
| TNF-α |

These Tables list key protein targets and ligands in this article which are hyperlinked to corresponding entries in http://www.guidetopharmacology.org, the common portal for data from the IUPHAR/BPS Guide to PHARMACOLOGY (Pawson *et al.*, 2014) and are permanently archived in the Concise Guide to PHARMACOLOGY 2013/14 ([a,b,c,d]Alexander *et al.*, 2013a,b,c,d).

## Introduction

Experimental autoimmune encephalomyelitis (EAE) is a CNS disease during which an autoimmune inflammatory response causes the destruction of oligodendrocytes, resulting in axonal demyelination. Overall, EAE in animals has proved a highly valuable tool for understanding the pathology of multiple sclerosis (MS) in humans (Batoulis *et al.*, 2011; Ransohoff, 2012). CD4+ Th1 and Th17 cells have been regarded as the main culprits in the pathogenesis. However, recent studies revealed that MS is also mediated by B-cells (DiLillo *et al.*, 2011). B-cells and their products have the capability to promote cellular immune responses. B-cells also present antigens as efficiently as other professional antigen-presenting cells, such as dendritic cells, and function as cellular adjuvants to promote CD4+ T-cell activation, expansion, memory formation and cytokine production *in vivo*. Thus, B-cells are generally considered as positive regulators of the immune response in an inflammatory context. However, IL10-producing, $CD5+CD1d^{high}$ B cells (named B10 cells) have been described as potent negative regulators in both mouse and humans (Matsushita *et al.*, 2008; Iwata *et al.*, 2011). In addition to B10 cells, other B-cell subsets therefore from the B2 lineage, such as transitional 2 (T2) or marginal zone (MZ) B-cells, have been proposed as having suppressive activities. Some regulatory B-cells (Bregs) originate therefore from the B2-cell lineage, although CD5+ B1 cells are also now known to have regulatory functions (DiLillo *et al.*, 2011; Mauri and Bosma, 2012; Kalampokis *et al.*, 2013).

Thus far, cell-specific markers for Bregs, analogous to the expression of the transcription forkhead box protein P3 (FoxP3) by regulatory T-cells (Tregs), have been difficult to establish. At present, the Bregs phenotype is not well defined in EAE (Mauri and Blair, 2010; Kalampokis *et al.*, 2013). However, a comparison of B-cell subsets from susceptible and resistant mice revealed that transitional B-cells are a characteristic feature of EAE (Lee-Chang *et al.*, 2011a). These results were also observed in early phases of MS (Lee-Chang *et al.*, 2011b).

The sigma receptors or binding sites (σ proteins), initially described as a subtype of opiate receptors, are now considered as unique receptors. Pharmacological studies have distinguished two types of σ proteins, termed σ1 and σ2. The σ1 type is an intracellular protein identified as a ligand-regulated molecular chaperone. This 25 kDa protein is present on mitochondrion-associated endoplasmic reticulum (ER) membranes. σ1 agonists potently modulate intracellular $Ca^{2+}$ mobilizations and extracellular $Ca^{2+}$ influx, in addition to numerous neurotransmitter responses, and result in activation of signalling pathways (Cobos *et al.*, 2008). In the CNS, this protein is expressed in neurons and oligodendrocytes. The σ1 protein has been shown to affect the action potential process by several modes of action. Indeed, the σ1 protein directly or indirectly modulates voltage-gated ion channels, glutamate and GABA ionotropic receptors, dopamine $D_1$ receptors, muscarinic and nicotinic ACh receptors and neurotrophic tyrosine kinase receptor type 2 (TrkB). The σ1 protein also interacts with intracellular targets such as kinases and inositol trisphosphate receptors (Kourrich *et al.*, 2012). Eliprodil, a high affinity but non-selective σ1 protein ligand with neuroprotective properties also modulated myelination by increasing the amount of myelinated axon segments (Demerens *et al.*, 1999). The σ1 protein is also expressed on lymphocytes, but the significance of this protein in the immune system has been poorly studied. The σ1 protein exhibits a well-established pharmacological profile, with high-affinity synthetic ligands. *In vitro*, specific σ1 protein ligands inhibit the proliferative responses of mouse $CD3^+$ lymphocytes. *In vivo*, they inhibit LPS-induced systemic release of IL-1, IL-6, TNF-α and IFN-γ and, interestingly, they can also enhance IL-10 release (Casellas *et al.*, 1994; Bourrie *et al.*, 1995; Derocq *et al.*, 1995).

A synthetic, high-affinity and selective ligand for the σ1 protein, compound 1(S), contains the tetrahydroisoquinoline-hydantoin structure, a limited number of free rotation bonds and a very low cytotoxicity providing a high selectivity index (ratio $CC_{50}/IC_{50}$), greater than 50 000 (Cazenave Gassiot *et al.*, 2005; Charton *et al.*, 2005; Toussaint *et al.*, 2010). It also has an agonist profile in cocaine-induced hyperlocomotion and locomotor sensitization (Toussaint *et al.*, 2009). In the present study, we have investigated the effect of compound 1(S) on the initiation and clinical development of EAE. Our data have shown that a single injection of compound 1(S) decreased the severity of EAE (clinically and histologically) by a σ1-dependent mecha-

nism, an effect that was associated with an increase of potential immunoregulatory transitional 2 (T2) B-cells as well as Tregs.

## Methods

### *Adsorption, diffusion, metabolism and excretion (ADME) assays*

Standardized *in vitro* ADME experiments were performed by CEREP (Paris, France). The bioavailability-related profile was measured according to Lipinski *et al.* (2001) for aqueous solubility (in PBS pH 7.4), Sangster (1997) for partition coefficient (logD, n-octanol : PBS, pH 7.4), Banker *et al.* (2003) for plasma protein binding, Grès *et al.* (1998) for A-B intestinal permeability (using TC7 cells, pH 6.5/7.4) and Kuhnz and Gieschen (1998) for metabolic stability (human liver microsomes). In parallel, inhibition of cytochrome P450 isoforms was evaluated according to Crespi *et al.* (1997) for cytochrome 1A2 and cytochrome 2C9, Ono *et al.* (1996) for cytochrome 2C19 and cytochrome 2D6, and Stresser *et al.* (2000) for cytochrome 3A4. The LC/MS system for microsomal stability and metabolite identification consisted of an Orbitrap Exactive instrument (Thermo Scientific, Waltham, MA, USA) equipped with an electrospray ionization source used in positive mode ($M+H^+$). The apparatus was managed with Xcalibur software. Inhibition of cloned hERG potassium ion channel repolarization was evaluated in CHO cells, according to Mathes (2006).

### *Animals*

All animal care and experimental procedures complied with the European Communities Council Directives of 24 November 1986 (86/609/EEC) and were approved by the local ethical committee (CEEA 102009R). Efforts were made to minimize the number of animals used and their suffering. Animals that reached severe hind limb paresis (clinical grade 3) were isolated, and hydration and food access were facilitated. All studies involving animals are reported in accordance with the ARRIVE guidelines for reporting experiments involving animals (Kilkenny *et al.*, 2010; McGrath *et al.*, 2010). A total of 103 animals were used in the experiments described here. SJL/J mice were purchased from Janvier (Le Genest-St-Isle, France) and bred under conventional barrier protection at the Pasteur Institute (Lille, France).

### *EAE induction and treatment*

The method of EAE induction has been described earlier (Lee-Chang *et al.*, 2011a). Randomized 9-week-old female SJL/J mice were inoculated s.c. in the neck with an emulsion containing 100 µg of myelin proteolipid protein $(PLP)_{139–151}$ peptide and an equal volume of complete Freund's adjuvant (CFA) containing 4 $mg·mL^{-1}$ of heat-inactivated *Mycobacterium tuberculosis* H37RA (Difco Laboratories, Detroit, MI, USA) on day 0 (D0). Additionally, mice received 0.3 µg of *Bordetella pertussis* toxin (BPT; Sigma-Aldrich, Saint Louis, MI, USA) i.p. on D0 and D3. Sham animals only received saline injection. SJL/J mice that only received CFA and BPT were also included in the experiments. Control animals received one administration of saline solution (EAE-vehicle or sham-vehicle mice). Mice showed no apparent toxic side effects of any of the treatment protocols.

### *Clinical evaluation*

Body weight and clinical signs of EAE were monitored daily. Three different treatment groups (EAE-vehicle, EAE-1(S) 1 $mg·kg^{-1}$ and EAE-1(S) 5 $mg·kg^{-1}$) were used per experiment, with 5–7 animals per treatment group. Data were compiled from three independent experiments ($n$ = 15–19 per group; Baker and Amor, 2012). The severity of clinical symptoms was scored based on a standard neurological scoring system for EAE, as follows: grade 0, no disease; grade 1, moderate tail hypotonia and/or slightly clumsy gait; grade 2, tail atony and/or clumsy gait; grade 3, severe hind limb paresis; grade 4, paraplegia; grade 5, tetraplegia; and grade 6, dead. Scoring was performed without knowledge of the treatments. Based on the clinical score data, EAE was characterized using the following parameters: incidence, cumulative disease index (CDI), disease peak, score at D14 ± 2, relapse duration and mortality. Incidence of EAE corresponds to the frequency of the new cases reaching grade 2. The CDI was calculated as the sum of the daily clinical scores for each mouse (Bodhankar *et al.*, 2011). Disease peak refers to the first day of maximal clinical score and relapse duration refers to the number of days that mice presented a clinical score ≥2. To ensure a maximum effect of compound 1(S), the next experiments were carried out at a dose of 5 $mg·kg^{-1}$.

### *Serum anti-PLP ELISA*

Mice were deeply anaesthetized with an i.p. injection of pentobarbital. Serum samples were prepared from peripheral blood obtained by cardiac puncture immediately before perfusion. Active immunizations were confirmed by measuring anti-$PLP_{139–151}$ IgG antibody (Ab), as previously described (El Behi *et al.*, 2007).

### *Isolation of mononuclear cells*

After blood sampling, mice were perfused with an intracardiac injection of chilled PBS. Spleen and cervical lymph nodes (CLNs) were isolated. Cell suspensions were obtained by mechanical dissociation using a nylon mesh of 80 µm (Millipore, Billerica, MA, USA) followed by incubation with erythrocyte lysis reagent (155 mM $NH_4Cl$, 10 mM $KHCO_3$ and 0.1 mM EDTA).

### *Measurement of cytokines*

Serum cytokines were measured using a mouse cytokine-plex assay kit (Bio-Rad, Hercules, CA, USA) with Bio-Plex Manager software version 6.0 in a Bio-Plex TM 200 system (Bio-Rad). This system allows quantitative measurement of IFN-γ, TNF-α, IL-17a and IL-4. Cytokines were evaluated according to the manufacturer's instructions. Four different groups (sham-vehicle; sham-1(S) 5 $mg·kg^{-1}$; EAE-vehicle and EAE-1(S) 5 $mg·kg^{-1}$) were used with 5–11 animals per treatment group.

### *Flow cytometry*

Briefly, phenotypic analysis of B1a (CD19+ CD5+ CD43+), MZ (CD19+ CD21high CD23–), transitional 2 (T2) (CD19+ CD93+ CD23+) or follicular (FO) (CD19+ CD21+, CD23high)

B-cell subsets and Tregs (CD4+ CD25+ FoxP3+) was performed with the appropriate combination of Abs allowing subset identification, as previously described (Lee-Chang *et al.*, 2011a). Isotype-matched negative controls were used throughout all studies. Cells were analysed using a FACSAria flow cytometer and Cell Quest software (BD Bioscience, Becton Dickinson and Company, Franklin Lakes, NJ, USA). Two independent studies were performed. Four different groups (sham-vehicle; sham-1(S) 5 mg·kg$^{-1}$; EAE-vehicle and EAE-1(S) 5 mg·kg$^{-1}$) were used per experiment, with four animals per group (Baker and Amor, 2012).

### Histology

After spleen and CLN isolation, mice were intracardially perfused with 4% paraformaldehyde (Carlo Erba Réactifs (SDS), Val-de-Reuil, France) solution in saline. Brain and spinal cord were removed, post-fixed for at least 4 h in the same fixative followed by 12 h in 20% sucrose solution before being embedded in ice-cold OCT (Optimal Cutting Temperature embedding medium, Cell Path, Newtown, UK), frozen in isopentane (–55°C), and stored at –80°C until sectioning.

Using a cryostat, 12 µm serial coronal sections from five levels of the neuroaxis (corpus callosum/striatum, cerebellum/brainstem, cervical, thoracic and lumbar spinal cords) were cut and collected on Superfrost/Plus slides (Thermo Scientific) and kept at –80°C until use. Brain and spinal cord sections were stained by conventional haematoxylin and eosin (H&E) or luxol fast blue (LFB) and examined by light microscopy, without knowledge of the treatments. Inflammation was quantified by counting the mononuclear cell infiltration foci (at least 20 clustered mononuclear cells) in the meninges and parenchyma by a double-blinded investigator. An arbitrary score from 0 to 4 was determined as follows: 0, no mononuclear cell infiltration; 1, few cellular infiltrates in perivascular and/or meninges area; 2, mild cellular infiltrates (≤10); 3, moderate cellular infiltrates (11–20); 4, severe cellular infiltrates (>20). The mean histological score was calculated for each group. Two groups (EAE-vehicle and EAE-1(S) 5 mg·kg$^{-1}$) were used in this experiment, with three animals per experimentation group. A total of 24 sections per CNS area per animal were analysed.

### Data analysis

Data are presented as median and interquartile range (IQR) due to the small size of the animal groups. Clinical parameters were analysed between the three groups (EAE-vehicle, EAE-1(S) 1 mg·kg$^{-1}$ and 5 mg·kg$^{-1}$) using a Kruskal–Wallis test, following *post hoc* pairwise comparisons using a Mann–Whitney *U*-test for continuous parameters and by Fisher's exact test for qualitative parameters. The clinical score evolution was compared between the three groups with a linear mixed model. This model is an extension of the classical ANOVA taking into account the correlation between measurements of the same subject. The fixed effects were the groups and the time. The random effect was the mice. For each CNS-area H&E analysis, the effect of administration of compound 1(S) on mononuclear cell infiltration was assessed by a linear mixed model in order to take into account that several sections were measured for each animal. The effect of administration of compound 1(S) on cytokine production was studied using a Student's *t*-test. The effect of compound 1(S) on T2, MZ, B1a, FO B-cells and Tregs in spleen and CLNs was assessed using a Kruskal–Wallis test. *Post hoc* analyses were performed using a Mann–Whitney *U*-test. Statistical analyses were performed using SAS software (SAS Institute, Cary, NC, USA; version 9.2). *P*-values <0.05 were considered statistically significant.

### Materials

Compound 1(S) was synthesized according to a previously reported protocol (Toussaint *et al.*, 2010). BD1047 (N-[2-(3,4-dichlorophenyl)ethyl]-N-methyl-2-(dimethylamino) ethylamine hydrochloride) was supplied by Tocris (Bristol, UK). All drugs were dissolved in physiological saline and injected i.p. on D0 in a volume of 100 mL per 20 g of body weight. Doses refer to the salt form. For antagonism studies, BD1047 was administered 20 min before compound 1(S).

## Results

### In vitro *ADME properties*

A range of physicochemical and biochemical properties of compound 1(S) (Figure 1), including aqueous solubility, logD, cell permeability and effects on CYP isoforms, were measured *in vitro* using methods already referred to in the Methods. The values obtained are listed in Table 1. Although compound 1(S) was chemically stable, it was rapidly metabolised by human liver microsomes (Table 1) to demethylated and debenzylated compounds (data not shown). However at 10 mM, compound 1(S) did not inhibit of any of the CYP forms tested (Table 1). Cardiotoxicity was estimated using the predictor hERG test. The $IC_{50}$ for tail current inhibition was 0.55 µM for compound 1(S).

### *Attenuation of clinical, histological and biological EAE after compound 1 (S) injection*

As comparative analysis of B-cell subsets in susceptible and resistant mice at critical time points has demonstrated a homeostatic breakdown of T2 and MZ B-cells in EAE mice at disease peak, a single injection of compound 1(S) was given on D0, at the time of immunization (Lee-Chang *et al.*, 2011a). Thus, mice were actively immunized with $PLP_{139–151}$ in CFA and immediately injected either with vehicle (saline) or with

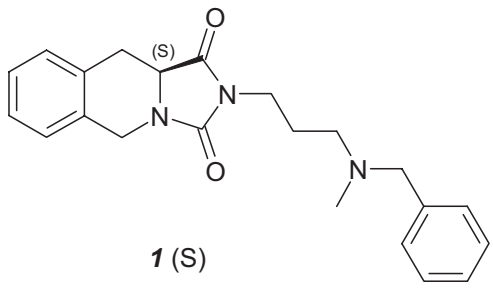


***1*** (S)

**Figure 1**

Chemical structure of compound 1(S), the σ1 protein agonist evaluated.

## Table 1

ADME profile of compound 1(S), the σ1 protein agonist used in these studies.

| | Values | Experimental conditions |
|---|---|---|
| Bioavailability | | |
| Aqueous solubility | 278 μM | PBS, pH 7.4 |
| logD | 2.15 | n-octanol/PBS, pH 7.4 |
| P-gp inhibition | 10.3% | 1 μM |
| Plasma protein binding | 93.1% (99.1% recovery) | 8 h, 37°C |
| A-B intestinal permeability ($10^{-6}$ cm·s$^{-1}$) | 53.6% (122% recovery) | TC7 cells, pH 6.5/7.4 |
| Metabolism study | | |
| Metabolic stability | 14% | 0 and 1 h, pH 7.4, 37°C human liver microsomes |
| CYP1A2 inhibition | –8% | CEC substrate, 10 μM |
| CYP2C9 inhibition | –1% | MFC substrate, 10 μM |
| CYP2C19 inhibition | 26% | CEC substrate, 10 μM |
| CYP2C6 inhibition | –30% | MFC substrate, 10 μM |
| CYP3A4 inhibition | 40% | BCF substrate, 10 μM |
| Toxicity | | |
| hERG, inhibition of tail current, $IC_{50}$ | 0.55 μM | |

compound 1(S) i.p. Three different groups, EAE-vehicle, EAE-1(S) 1 mg·kg$^{-1}$, and EAE-1(S) 5 mg·kg$^{-1}$, were used per experiment, with 5–7 animals per treatment group. The EAE disease course was followed for 35 days after immunization. Active immunization was confirmed by measuring the serum anti-$PLP_{139–151}$ IgG antibody at day 35 (D35; data not shown). Data were compiled from three independent experiments ($n$ = 15–19/group).

Clinical observation showed that EAE-vehicle (control) mice experienced onset of symptoms at D11 (Figure 2A). A single injection of compound 1(S) (1 or 5 mg·kg$^{-1}$) decreased the CDI ($P$ = 0.0246; Table 2). EAE-vehicle mice peaked at D13 and presented a maximal clinical score of 4.0 (Figure 2A; Table 2), as previously described (Tuohy *et al.*, 1989; Magliozzi *et al.*, 2004; Lee-Chang *et al.*, 2011a). However, compound 1(S) (1 or 5 mg·kg$^{-1}$) did not modify the disease peak ($P$ = 0.1287). In light of this, and in accordance with previous results, disease peak was fixed at D14 ± 2 for the subsequent analysis (Lee-Chang *et al.*, 2011a). The single injection of compound 1(S) (1 or 5 mg·kg$^{-1}$) reduced the clinical score at this critical point ($P$ < 0.0001). Compound 1(S) injection also significantly changed relapse duration ($P$ = 0.0003), without reducing mortality ($P$ = 0.1371) (Table 2). The effects of compound 1(S) were not dose-related, as there was no difference in the effects on any of the clinical parameters analysed, between 1 mg·kg$^{-1}$ and 5 mg·kg$^{-1}$ treatments. Nevertheless, linear mixed model statistical analysis showed that clinical scores were higher in EAE-vehicle mice compared with EAE-1(S) 1 or 5 mg·kg$^{-1}$ mice ($P$ = 0.007). The clinical scores remained significantly different over the 35 day experimental period ($P$ < 0.0001; Figure 2A).

To confirm that the biological activities of compound 1(S) required the presence of the σ1 protein, we blocked its binding sites with the σ1 protein antagonist BD1047, given i.p. (10 mg·kg$^{-1}$), 20 min before compound 1(S) (1 or 5 mg·kg$^{-1}$) (Meunier *et al.*, 2006). As shown in Figure 2B, BD1047 blocked the effects of compound 1(S) (5 mg·kg$^{-1}$) on EAE initiation and development. No significant difference was observed when we compared the median clinical score of EAE-vehicle and EAE-BD1047 and 1(S) 5 mg·kg$^{-1}$ mice at disease peak, that is, D14 ± 2 ($P$ = 0.0917), even when a significant difference was observed after compound 1(S) injection ($P$ = 0.0012). Similar results were obtained with compound 1(S) injected at 1 mg·kg$^{-1}$. BD1047 alone displayed no significant effects on EAE (data not shown).

Analysis of cellular infiltration and demyelination were also performed at D14 ± 2 in EAE-vehicle mice (clinical grade 4.0) and EAE-1(S) 5 mg·kg$^{-1}$ mice (clinical grade 1.5; Figure 2A) (Table 2). An extensive analysis of the CNS was performed using smples of the corpus callosum/striatum, cerebellum/brainstem, and the cervical, thoracic and lumbar spinal cord (Figure 3). Figure 3A shows that EAE-vehicle mice were characterized by infiltration of mononuclear cells in the corpus callosum/striatum (mean scores are shown in Figure 3A), mainly meningeal (Figure 3B, panels A and B). The cell infiltration was higher in the cerebellum and brainstem (Figure 3A); it was characterized by meningeal and perivascular parenchymal infiltrates (data not shown). No differences were observed between the histological scores of cervical, thoracic and lumbar spinal cord. Lesions were typically located within the CNS white matter (Figure 3B, panels D and E). In EAE-1(S) 5 mg·kg$^{-1}$ mice, histological analyses revealed that the infiltrating mononuclear cell foci score was not significantly changed in the corpus callosum/striatum, but was reduced in the cerebellum and brainstem ($P$ < 0.005). Inflamed vessels were never found in the cervical, thoracic and lumbar spinal cord of EAE-1(S) 5 mg·kg$^{-1}$ mice ($P$ < 0.005). Panels C and F of Figure 3B show signifi-

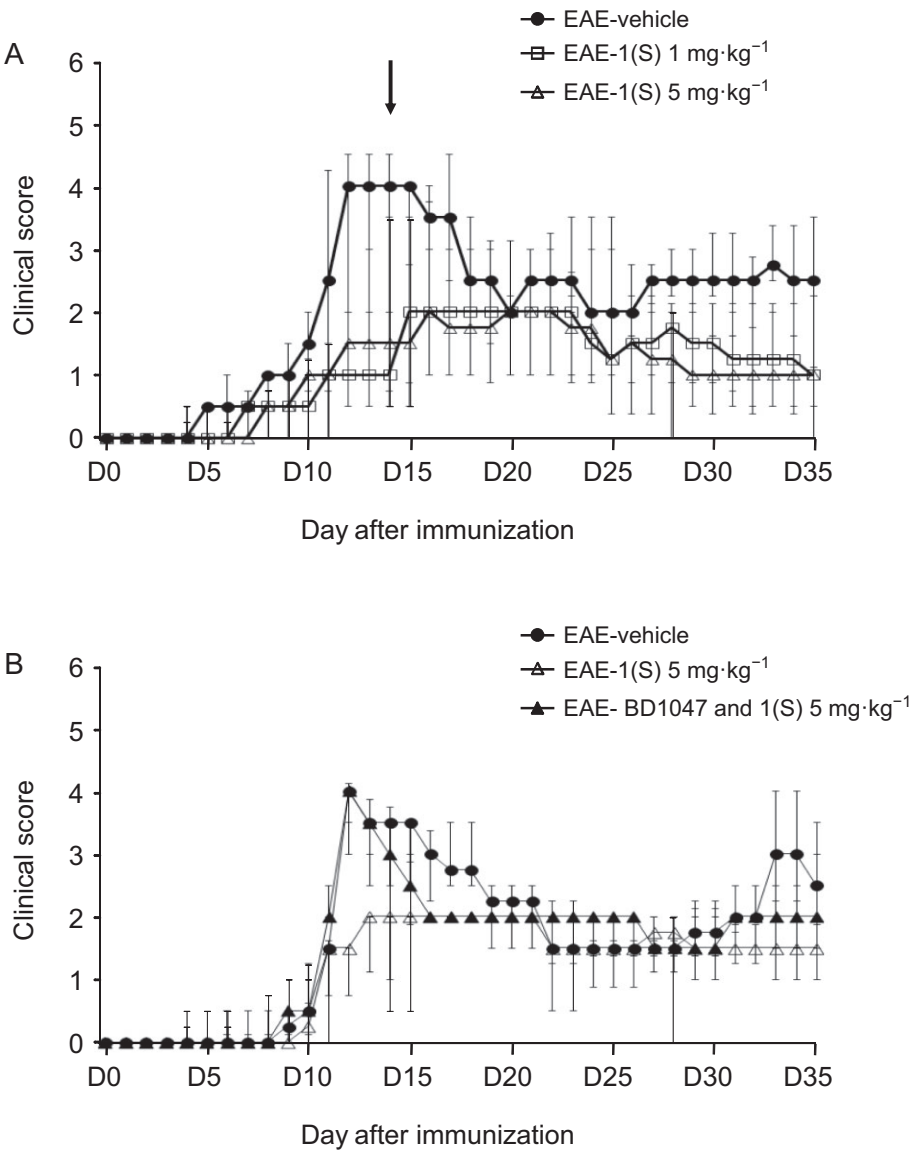


## Figure 2

Effect of compound 1(S) on clinical signs of PLP $_{139–151}$-induced EAE in SJL/J mice. Mice were immunized on day 0 (D0) and their clinical course was followed for the next 35 days. Data are presented as median ± inter-quartile range IQR. (A) Reduction of EAE clinical score by a single injection of compound 1(S) at D0. Three different groups, EAE-vehicle, EAE-1(S) 1 mg·kg$^{-1}$ and EAE-1(S) 5 mg·kg$^{-1}$, were used per experiment with 5–7 animals per treatment group. Data were compiled from three independent experiments ($n$ = 15–19/group). The arrow indicates the time corresponding to the disease peak, when the histological, Tregs and B-cell subsets analyses were carried out. (B) Involvement of the σ1 protein in the beneficial effects of compound 1(S) on the clinical scores. Three different groups, EAE-vehicle, EAE-1(S) 5 mg·kg$^{-1}$ and EAE-BD1047 and 1(S) 5 mg·kg$^{-1}$ were used per experiment with nine animals per treatment group. The σ1 protein antagonist BD1047 (10 mg·kg$^{-1}$) was given i.p., 20 min before compound 1(S) injection. Data are from two separate experiments.

cantly attenuated cellular infiltration in the brain parenchyma and spinal cord of EAE-1(S) 5 mg·kg$^{-1}$ animals. Analysis of myelin content by LFB staining was also performed at the same time as H&E staining, using serial sections. Demyelination was confirmed in EAE-vehicle mice, mainly in the spinal cord (Figure 3B, panels J and K). Meningeal cuffs observed in the corpus callosum/striatum and cerebellum/brainstem did not lead to demyelination in EAE-vehicle mice (Figure 3B, panels G and H). EAE-1(S) 5 mg·kg$^{-1}$ mice showed no demyelination in the corpus callosum/striatum, cerebellum/brainstem or spinal cord (Figure 3B, panels I and L).

To analyse whether the clinical and histological modulation of EAE observed after the single injection of compound 1(S) could be correlated with the modulation of the peripheral inflammatory state, five serum cytokines were also assayed in sham-vehicle, sham-1(S) 5 mg·kg$^{-1}$, EAE-vehicle and EAE-1(S) 5 mg·kg$^{-1}$ mice at D14 ± 2 after immunization.

## Table 2

Effect of the σ1 protein agonist, compound 1(S), on EAE development[a]

| | Incidence | CDI | Disease peak | Score at D14 ± 2 | Relapse duration | Mortality |
|---|---|---|---|---|---|---|
| EAE-vehicle | 15/15 | 71.2 (±44.5) | D13 (±4) | 4.0 (±1.0) | 21 (±13.5) | 6/15 |
| EAE-1(S) 1 mg·kg$^{-1}$ | 15/19 | 45.5 (±35.8)* | D16 (±6) | 1.0 (±0.5)*** | 7.5 (±17.0)* | 2/19 |
| EAE-1(S) 5 mg·kg$^{-1}$ | 14/19 | 40.0 (±34.3)* | D16 (±5) | 1.5 (±0.5)*** | 7.5 (±11.0)* | 3/19 |

[a]To evaluate the effect of compound 1(S) on EAE development, we used three different groups, EAE-vehicle, EAE-1(S) 1 mg·kg$^{-1}$ and EAE-1(S) 5 mg·kg$^{-1}$. Data were compiled from three independent experiments with 5–7 animals per group ($n$ = 15–19/group). Incidence corresponds to the frequency of the new cases reaching clinical grade 2. CDI was calculated as the sum of the daily clinical scores for each mouse (Bodhankar *et al.*, 2011). Disease peak refers to the first day of maximal clinical score. Relapse duration refers to the number of days that mice showed a clinical score ≥2. Data are presented as median ± IQR. No significant differences were observed between any of the effects of 1 mg·kg$^{-1}$ and 5 mg·kg$^{-1}$ compound 1(S). *$P$ < 0.05, ***$P$ < 0.0005; significantly different from the EAE-vehicle group.

The results were inconclusive as to whether a single injection of compound 1(S) at D0 did modulate serum cytokine production (Supporting Information Table S1).

### *Modulation of Foxp3+ Tregs and B-cell subsets after compound 1(S) injection*

CD4+ CD25+ Foxp3+ Tregs depress the autoimmune response causing EAE (O'Connor and Anderton, 2008). Breakdown of T2 and MZ B-cells was observed in susceptible EAE mice at disease peak (D14 ± 2), compared with resistant mice (Lee-Chang *et al.*, 2011a). Tregs and B-cell subsets were analysed in sham-vehicle, sham-1(S) 5 mg·kg$^{-1}$, EAE-vehicle and EAE-1(S) 5 mg·kg$^{-1}$ mice, in spleen and brain-draining CLNs at D14 ± 2 after immunization.

As illustrated in Figure 4, in the spleen of sham-vehicle and EAE-vehicle mice, immunization did not modify the amount of Foxp3+ Tregs 14 days after EAE development (Figure 4A). A slight increase in the number of Tregs was observed at the draining site after PLP immunization (i.e. CLNs; Figure 4B). Immunization with CFA-TBP alone had no effect on the number of Tregs (data not shown). On the contrary, a comparison of sham-vehicle vs. sham-1(S) 5 mg·kg$^{-1}$ and EAE-vehicle vs. EAE-1(S) 5 mg·kg$^{-1}$ mice demonstrated that a single injection of compound 1(S) at D0 increased Treg numbers in the spleen 14 days after EAE development in both sham and EAE mice (Figure 4A; sham, $P$ = 0.0198 and EAE $P$ = 0.004). Similar results were observed in CLNs [Figure 4B; sham $P$ = 0.001 and EAE, $P$ = 0.039).

EAE-vehicle mice showed significantly reduced MZ and FO B-cell counts in their spleen 14 days after EAE development (Figure 5B and D; MZ, $P$ = 0.042 and FO, $P$ = 0.021). A less marked decrease was noted for B1a B-cells in EAE-vehicle mice (Figure 5C; $P$ = 0.093). An accumulation of B1a and FO B-cells was observed in the CLNs of EAE-vehicle mice 14 days after EAE development (Figure 6A and B; B1a,, $P$ = 0.015 and FO, $P$ = 0.018). Treatment with compound 1(S) (5 mg·kg$^{-1}$) of sham or EAE mice did not affect MZ, B1a or FO B-cell numbers in the spleen (Figure 5B–D) but induced a specific increase in T2 B-cells (Figure 5A; sham, $P$ = 0.003 and EAE, $P$ = 0.0003). However, in the CLNs, compound 1(S) injection did not modify B1a or FO B-cell counts in sham and EAE mice (Figure 6A and B).

## Discussion

In mice, EAE exhibits histopathological changes characterized by infiltration of the CNS by peripheral leukocytes, including autoimmune deleterious T- and B-cells, reactive gliosis, demyelination and substantial axonal loss (Brown *et al.*, 1982). The damaged areas observed are similar to those found in active plaques of MS patients. However, there are different gradients in the severity of inflammation and demyelination depending on the mouse strain used. In this study, SJL/J mice were used as severe inflammation is observed in this strain (Dal Canto *et al.*, 1995). Furthermore, this experimental model is a chronic disease with a spontaneous pattern of relapse and remissions (R-EAE), comparable with the most common form of MS (Webb *et al.*, 2004; Ransohoff, 2012). It has already been demonstrated that specific σ1 protein ligands inhibit CD3+ lymphocytes proliferation and LPS-induced release of IL-1, IL-6, TNF-α and IFN-γ, and can enhance LPS-induced release of IL-10 (Casellas *et al.*, 1994; Bourrie *et al.*, 1995; Derocq *et al.*, 1995). The aim of this study was thus to observe the potential role of a σ1 protein agonist on inflammatory processes, particularly in EAE. As B-cells are also known as immunocompetent cells with deleterious and/or beneficial effects in EAE and MS pathogenesis, and as homeostatic breakdown of B-cell subsets has been associated with the induction of EAE (Mann *et al.*, 2012), we decided to inject compound 1(S) at immunization time (D0). Compound 1(S) was injected at 1 and 5 mg·kg$^{-1}$, two concentrations within a range of σ protein ligands previously tested (Casellas *et al.*, 1994; Derocq *et al.*, 1995; Demerens *et al.*, 1999; Fujino *et al.*, 2003; Toussaint *et al.*, 2009).

No time lag was observed for EAE disease peak in vehicle or in treated mice, but injection of compound 1(S) significantly reduced EAE intensity. Consequently, histological analysis of the CNS was performed 14 ± 2 days after immunization, which corresponds to the disease peak and the time that major mononuclear cell infiltrations were observed in EAE mice (Tuohy *et al.*, 1989; Lee-Chang *et al.*, 2011a). Immunostaining for σ1 protein has been observed throughout the rostrocaudal regions of the CNS, extending from the olfactory bulb to the spinal cord in adult rodents (Alonso *et al.*, 2000). However, the cerebellum presents more specific σ1 protein

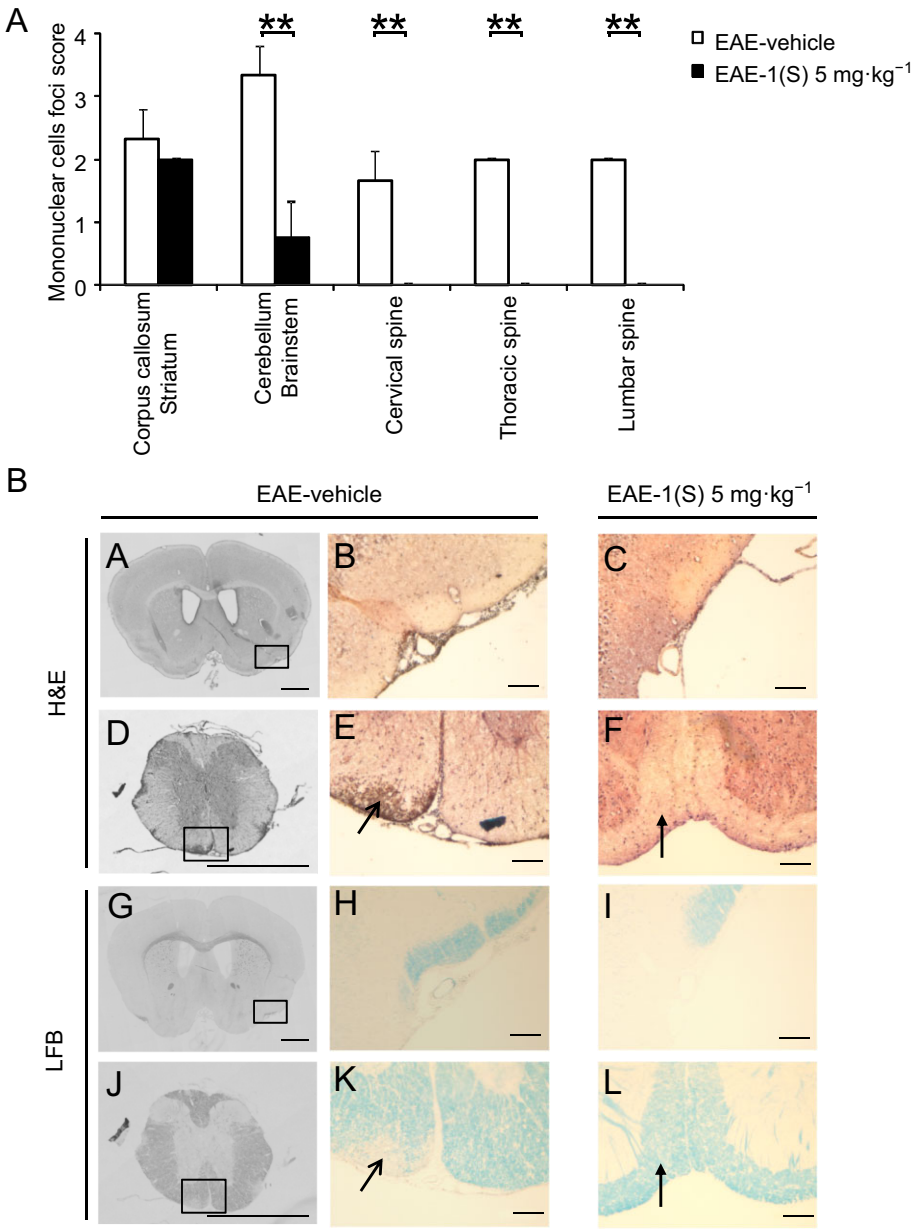


## Figure 3

A single injection of compound 1(S) at D0 decreased the infiltration of mononuclear cells and the demyelination in the corpus callosum and the spinal cord in EAE mice. Two different groups, EAE-vehicle and EAE-1(S) 5 mg·kg$^{-1}$ were used. Mice were immunized to induce EAE and compound 1(S) (5 mg·kg$^{-1}$) given i.p. Animals were killed at the peak of disease (i.e. on day 14 ± 2), when the clinical grade for the EAE-vehicle group was 4.0 and for the EAE-1(S) 5 mg·kg$^{-1}$ group was 1.5. This experiment utilized three animals per experimentation group. A total of 24 sections per CNS area per animal were analysed. (A) Quantification of mononuclear cell infiltration in corpus callosum/striatum, cerebellum/brainstem, and cervical, thoracic and lumbar spine. Graph bars indicate the inflammatory score (means ± SD). $^{**}P < 0.005$, significantly different as indicated. (B) Representative light microscopy of mouse corpus callosum/striatum (panels A–C, G–I) or spinal cord (panels D–F, J–L) sections stained with H&E or LFB. Only EAE-vehicle mice show moderate and extensive inflammatory lesions, in corpus callosum (panels A and B) and spinal cord (panels D and E open arrowhead) respectively. Sections from the same level stained for myelin show loss of myelin in the spinal cord (panels J and K open arrowhead), while white matter was not disrupted in the corpus callosum/striatum area (panels G and H). Minimal infiltration (panels C and F filled arrowhead) and no demyelination (panels I and L filled arrowhead) was observed in sections from EAE-1(S) mice. Scale bars = 100 μm, original magnification: 10×.

binding sites than the corpus callosum (Bouchard and Quirion, 1997). Spinal cord, cerebellum and forebrain correspond to areas affected early after the increase of blood–brain-barrier (BBB) permeability (Cross *et al.*, 1993). Consequently, an analysis of the CNS was performed from the corpus callosum/striatum to the lumbar spinal cord in EAE-vehicle mice (clinical grade 4.0) and EAE-1(S) 5 mg·kg$^{-1}$ mice (clinical grade 1.5). Mononuclear cell infiltrations were attenuated in

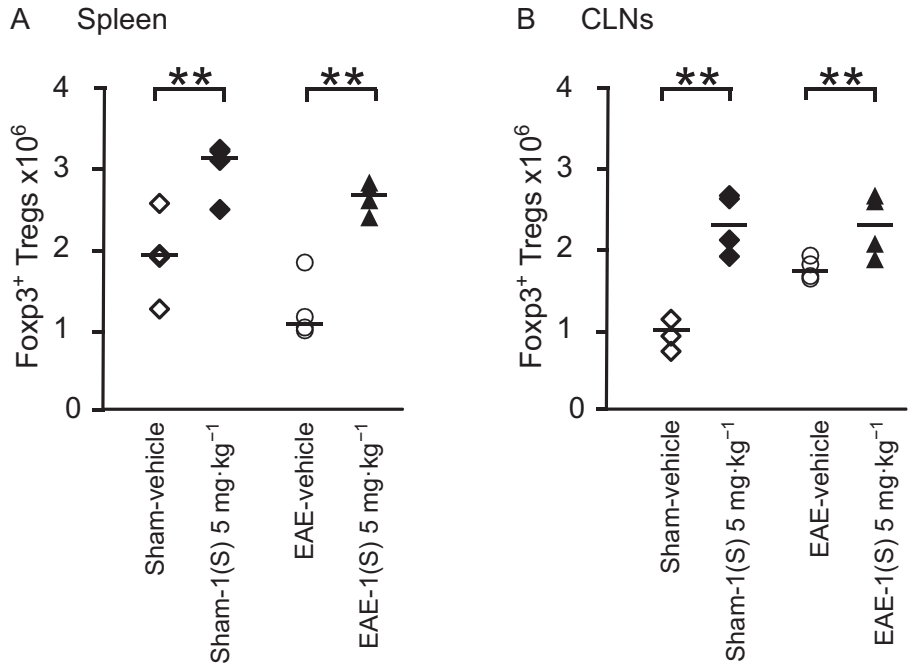


## Figure 4

Foxp3+ regulatory T-cells are increased in spleen and CLNs by a single injection of the σ1 protein agonist on D0. Foxp3+ Tregs (A and B) counts were analysed in spleen and CLNs in sham and EAE mice. Compound 1(S) (5 mg·kg$^{-1}$) was given i.p. Animals were killed at the peak of disease (i.e. on day 14 ± 2) after immunization (clinical grades: sham-vehicle and sham-1(S) 5 mg·kg$^{-1}$ group, 0; EAE-vehicle, 4.0; EAE-1(S) 5 mg·kg$^{-1}$ group, 1.5). Horizontal bar indicates median values. $^{**}P < 0.005$, significantly different as indicated. This experiment utilized four animals per experimentation group and is representative of two independent studies.

the cerebellum/brainstem area and absent in the spinal cord of treated mice. It has been suggested that classical EAE models might not be the most suited for studies of myelin repair (Baker and Amor, 2012). However, the most severe lesions are observed in SJL/J mice and primary demyelination is localized around some of the perivascular cuffs (Tuohy *et al.*, 1989; Dal Canto *et al.*, 1995). Therefore, we analysed myelination and mononuclear cell infiltration at the same time (Kozlowski *et al.*, 1987). As expected, little or no demyelination was observed in EAE-1(S) mice, in any of the areas tested.

EAE is characterized by inflammation and demyelination of the CNS. Priming of the myelin-specific response occurs in the secondary lymphoid organs, after which the pathogenic cells migrate to the CNS via the bloodstream. The vast majority of effector cells reside in the periphery and not in the target tissue, even at the EAE disease peak (Targoni *et al.*, 2001). Th1 and Th17 cells are pathogenic in EAE and possibly in MS. Th2 cells are thought to be protective. Cytokines such as IL-4, IL-10 and IL-5 have been associated with inflammation reduction and improvement of symptoms in EAE (El Behi *et al.*, 2010). No modulation of serum levels of cytokines was observed in this study, compatible with the restriction of the major effects of cytokines to the target organ, during autoimmune pathogenesis. As Foxp3+ Tregs represent a well-defined regulatory cell subset, their homeostasis was analysed at disease peak (D14 ± 2) after the single injection of compound 1(S). A significant increase of this subset was observed in the spleen and CLNs of sham-1(S) and EAE-1(S) animals. These results are in agreement with the involvement of Treg cells in autoreactive T-cell effector function and autoimmune disease progression suppression early in the induction of the auto-aggressive response, namely in the lymph nodes. Furthermore, in the PLP-induced model, the susceptibility of different mouse strains correlates inversely with the frequency of PLP-specific Tregs (Fletcher *et al.*, 2010). B-cell depletion could also modulate EAE initiation and disease progression (Matsushita *et al.*, 2008). Until now, identification of the binding sites on σ1 protein in lymphocytes has been performed using [$^3$H] high-affinity ligands (Coccini *et al.*, 1991). On the basis of previous data from our laboratory, B-cell subsets were also analysed in mice spleen and CLNs, after we had confirmed expression of σ1 protein in B lymphocytes (data not shown). Indeed, spleen performs an important immunological function but CLNs may be an important crossroad for processes taking place in the CNS during EAE. B1a, MZ, T2 and FO B-cells were also evaluated in spleen and CLNs to better understand their involvement in the immunological regulation that followed compound 1(S) injection. As expected, EAE led to a significant decrease of MZ and FO B-cells in the spleen. The reduction was less marked for the B1a B-cell subset. Interestingly, a significant increase in T2 B-cell numbers was observed in the spleen of sham-1(S) and EAE-1(S) animals. Indeed, the T2 and MZ B-cell subpopulations are exclusively located in this organ in rodents (Carsetti *et al.*, 2004). Concurrently, EAE significantly increased B1a and FO B-cell subsets in CLNs but no modulation was observed after compound 1(S) injection. T2-MZ

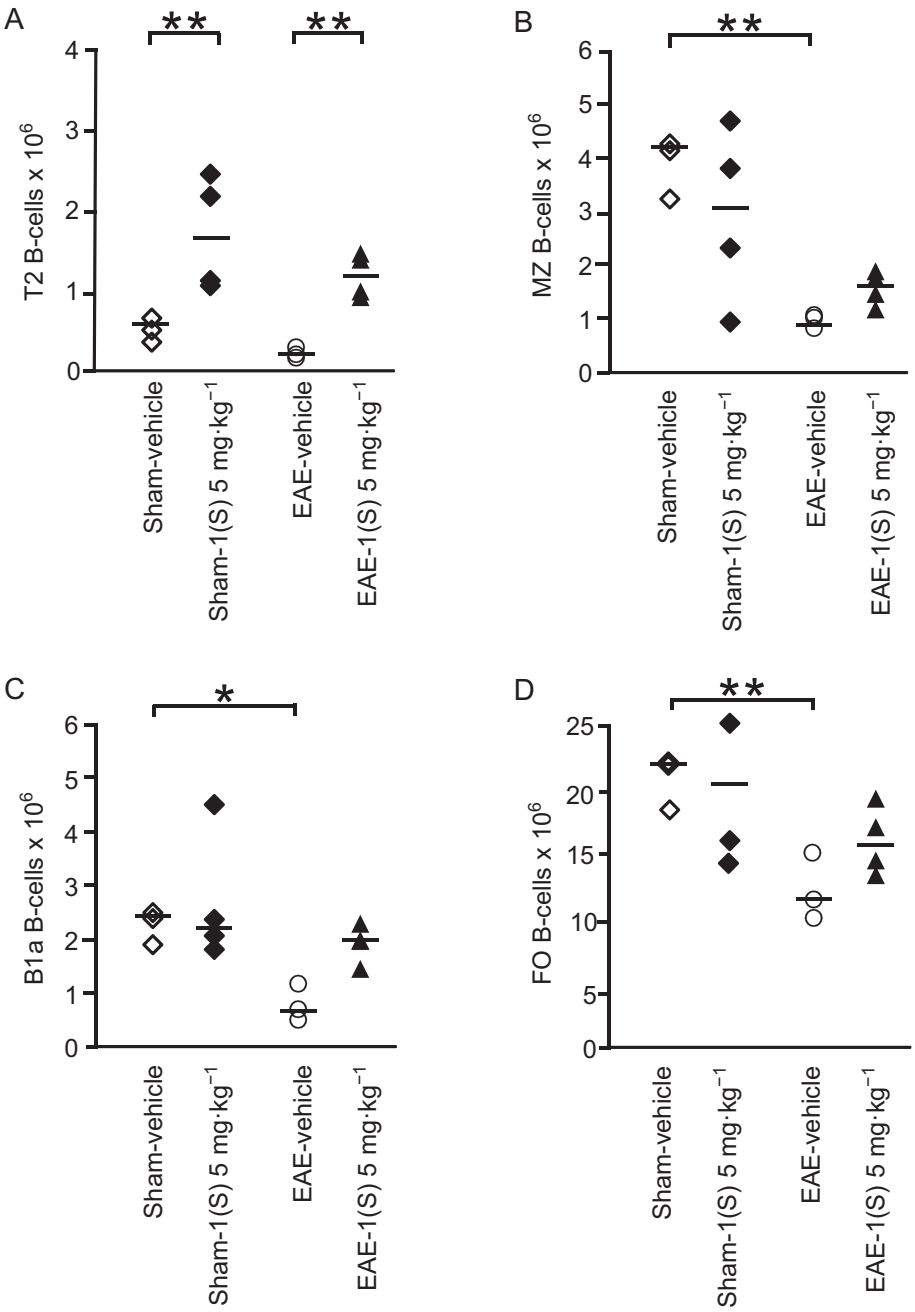


## Figure 5

Transitional 2 (T2) B-cell subset is increased in spleen by a single injection of the σ1 protein agonist on D0. T2 (A), MZ (B), B1a (C) and follicular, FO (D) B-cell sub-population counts were analysed in spleen in sham and EAE mice. Compound 1(S) (5 mg·kg$^{-1}$) was given i.p. Animals were killed at the peak of disease (i.e. on day 14 ± 2) after immunization (clinical grades: sham-vehicle and sham-1(S) 5 mg·kg$^{-1}$ group, 0; EAE-vehicle, 4.0; EAE-1(S) 5 mg·kg$^{-1}$ group, 1.5). Horizontal bar indicates median values. Significant differences are indicated as follows: *$P < 0.05$, **$P < 0.005$; significantly different as indicated. This experiment utilized four animals per experimentation group and is representative of two independent studies.

B-cells could potentially belong to the Bregs family as B10 cells and transitional 2 marginal-zone precursors (T2-MZP) Breg cells share common surface markers. Indeed, functional differences should exist between B10 cell progenitors ($B10_{pro}$), B10 and T2-MZP, T2 and MZ B-cell subsets (Mauri and Blair, 2010; Kalampokis *et al.*, 2013). Today, relatively few data are available to explain the precise role of transitional B-cells during EAE initiation and development. In mice, it appears that a slight homeostatic breakdown of T2 might be associated with the induction of and susceptibility to EAE and, as a consequence, with the emergence of pathogenic events (Lee-Chang *et al.*, 2011a). In humans, transitional or

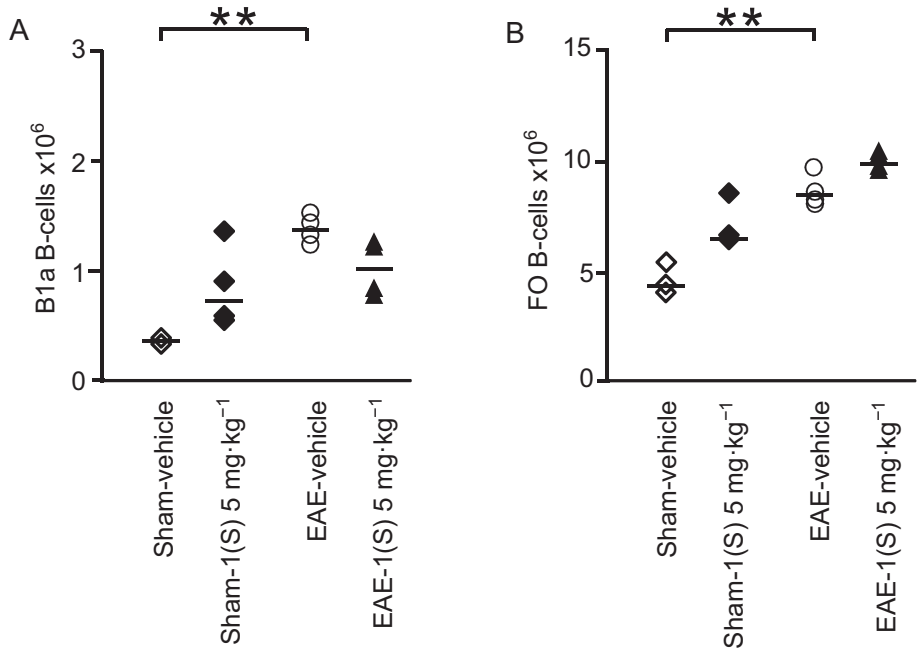


## Figure 6

No modulation of B-cell subsets in CLNs by a single injection of σ1 protein agonist on D0. B1a (A) and FO (B) B-cell sub-population counts were analysed in CLNs in sham and EAE mice. Compound 1(S) (5 mg·kg$^{-1}$) was given i.p. Animals were killed at the peak of disease (i.e. on day 14 ± 2) after immunization (clinical grades: sham-vehicle and sham-1(S) 5 mg·kg$^{-1}$ group, 0; EAE-vehicle, 4.0; EAE-1(S) 5 mg·kg$^{-1}$ group, 1.5). Horizontal bar indicates median values. $^{**}P < 0.005$, significantly different as indicated. This experiment utilized four animals per experimentation group and is representative of two independent studies.

'late-immature' B-cells, were considerably reduced in blood samples from MS patients (Lee-Chang *et al.*, 2011b).

The beneficial effect of σ1 protein agonists on the central neurodegenerative process is well documented. Eliprodil has the potential to increase myelination of CNS neurons *in vitro* (Demerens *et al.*, 1999). Dextrometorphan, a high-affinity σ1 protein agonist, inhibited, *in vitro*, the cytotoxic effects on oligodendroglia and oligodendroglial progenitors of several molecules that have been shown to be important in the pathogenesis of EAE (Lisak *et al.*, 2014). In the CNS, σ1 protein is also involved in the modulation of astrocytes, macrophages/microglia as well as in the increase of BBB permeability (Yao *et al.*, 2011). Nevertheless, neuroprotection without immunomodulation is not sufficient to reduce first relapse severity in EAE (Hasseldam and Johansen, 2010). The results obtained in this study confirm previous data highlighting the involvement of the σ1 protein in the immunological response. The mechanisms need to be examined in more detail, but the frequency of T2 B-cells and Tregs was clearly augmented by compound 1(S) regardless of the presence of inflammation.

It has been reported that specific ion channels or receptors are not affected by σ1 protein or ligands under normal physiological conditions. The assistance of σ1 chaperones seems to be solely required under pathological conditions (Su *et al.*, 2010). It would be interesting to analyse σ1 protein expression and distribution in EAE and sham animals, with or with out compound 1(S), as the accumulation of σ1 protein is a common finding in various neurodegenerative diseases and its localization at the ER and/or mitochondrion-associated ER membrane is affected by the pharmacological activation of this protein (Su *et al.*, 2010; Hedskog *et al.*, 2013; Miki *et al.*, 2014). Mutations of the σ1 protein gene have also been associated with amyotrophic lateral sclerosis and frontotemporal lobar degeneration (Peviani *et al.*, 2014).

The σ1 protein is involved in various acute and chronic pathologies, in cell survival as well as in cell proliferation. This ligand-regulated molecular chaperone has been described as an intracellular amplifier, creating a supersensitized state for signal transduction. The σ1 protein also affects mitochondrial $Ca^{2+}$ influx by stabilizing $IP_3Rs$ and acting as an inter-organelle signalling modulator of $Ca^{2+}$-homeostasis, ER stress reaction and apoptosis. Under prolonged stimulation, the σ1 protein interacts with several plasma membrane proteins, including voltage-dependent ($Na^+$, $K^+$, $Ca^{2+}$) and ligand-operated (NMDA) receptors, ion channels and kinases (Su *et al.*, 2010). All these partners play critical roles in regulating proliferation, cytokine production, cytotoxic function and *in vivo* migration of lymphocytes. The significant increase in Tregs and T2 B-cell numbers observed after compound 1(S) injection might also be partly attributable to their differential expression on B- and T-cell subsets (Chhabra *et al.*, 2014). Furthermore, apart from the modulation of the level of expression, cell subsets could also express a different profile of σ1 protein partners, depending on their activation states.

In summary, ADME analysis *in vitro* demonstrated that compound 1(S) was soluble, bioavailable, able to cross

biological barriers and presented little toxicity (Toussaint *et al.*, 2009). A single injection in EAE-susceptible mice at immunization time prevented mononuclear cell accumulation and demyelination in brain and spinal cord and increased T2 B-cells in the spleen and Tregs in spleen and CLNs, resulting in an overall reduction in the clinical progression of disease and confirming the involvement of σ1 protein in this immunological response. Nevertheless, compound 1(S) has only moderate metabolic stability and this has to be taken into account for the further development of new compounds sharing similar profiles.

## Acknowledgements

We thank M. Bellard for technical assistance, J. P. Decavel and T. Chassat for invaluable advice on animal manipulations and Dr C. Allet for histology knowledge and experience. We also thank S. Loiseaux, M. Delbeke and Dr A. Sarazin for multiplex assay knowledge and experience, G. Hochart for metabolite identification and Dr LT. Mars for fruitful discussions about the manuscript. We thank Université de Lille and particularly Lille 2 University for their financial support. This work was supported by BiogenIdec. The funding sources had no role in the study design, data collection and analysis, decision to publish or preparation of the manuscript.

## Author contributions

Conceived and designed the experiments: B. O., D. L., P. M., P. V. Performed the experiments: B. O., C. L. C., M. G., M. T., M. D. M. Analysed the data: B. O., A. D. Wrote the paper: B. O.

Critical revision of the manuscript for important intellectual content: C. L. C., L. P., P. M., P. V., P. C. , H. Z.

## Conflict of interest

The authors declare no competing financial interests.

## References

Alexander SPH, Benson HE, Faccenda E, Pawson AJ, Sharman JL, McGrath JC *et al.* (2013a). The Concise Guide to PHARMACOLOGY 2013/14: Overview. Br J Pharmacol 170: 1449–1458.

Alexander SPH, Benson HE, Faccenda E, Pawson AJ, Sharman JL, Spedding M *et al.* (2013b). The Concise Guide to PHARMACOLOGY 2013/14: G Protein-Coupled Receptors. Br J Pharmacol 170: 1459–1581.

Alexander SPH, Benson HE, Faccenda E, Pawson AJ, Sharman JL, Spedding M *et al.* (2013c). The Concise Guide to PHARMACOLOGY 2013/14: Catalytic Receptors. Br J Pharmacol 170: 1676–1705.

Alexander SPH, Benson HE, Faccenda E, Pawson AJ, Sharman JL, Catterall WA *et al.* (2013d). The Concise Guide to PHARMACOLOGY 2013/14: Ligand-Gated Ion Channels. Br J Pharmacol 170: 1582–1606.

Alonso G, Phan V, Guillemain I, Saunier M, Legrand A, Anoal M *et al.* (2000). Immunocytochemical localization of the sigma-1 receptor in the adult rat central nervous system. Neuroscience 97: 155–170.

Baker D, Amor S (2012). Publication guidelines for refereeing and reporting on animal use in experimental autoimmune encephalomyelitis. J Neuroimmunol 242: 78–83.

Banker MJ, Clark TH, Williams JA (2003). Development and validation of a 96-well equilibrium dialysis apparatus for measuring plasma protein binding. J Pharm Sci 92: 967–974.

Batoulis H, Recks MS, Addicks K, Kuerten S (2011). Experimental autoimmune encephalomyelitis – achievements and prospective advances. APMIS 119: 819–830.

Bodhankar S, Wang C, Vandenbark AA, Offner H (2011). Estrogen-induced protection against experimental autoimmune encephalomyelitis is abrogated in the absence of B cells. Eur J Immunol 41: 1165–1175.

Bouchard P, Quirion R (1997). [3H]1,3-di(2-tolyl)guanidine and [3H](+)pentazocine binding sites in the rat brain: autoradiographic visualization of the putative sigma1 and sigma2 receptor subtypes. Neuroscience 76: 467–477.

Bourrie B, Bouaboula M, Benoit JM, Derocq JM, Esclangon M, Le Fur G *et al.* (1995). Enhancement of endotoxin-induced interleukin-10 production by SR 31747A, a sigma ligand. Eur J Immunol 25: 2882–2887.

Brown A, McFarlin DE, Raine CS (1982). Chronologic neuropathology of relapsing experimental allergic encephalomyelitis in the mouse. Lab Invest 46: 171–185.

Carsetti R, Rosado MM, Wardmann H (2004). Peripheral development of B cells in mouse and man. Immunol Rev 197: 179–191.

Casellas P, Bourrie B, Canat X, Carayon P, Buisson I, Paul R *et al.* (1994). Immunopharmacological profile of SR 31747: in vitro and in vivo studies on humoral and cellular responses. J Neuroimmunol 52: 193–203.

Cazenave Gassiot A, Charton J, Girault-Mizzi S, Gilleron P, Debreu-Fontaine MA, Sergheraert C *et al.* (2005). Synthesis and pharmacological evaluation of Tic-hydantoin derivatives as selective sigma1 ligands. Part 2. Bioorg Med Chem Lett 15: 4828–4832.

Charton J, Cazenave Gassiot A, Girault-Mizzi S, Debreu-Fontaine MA, Melnyk P, Sergheraert C (2005). Synthesis and pharmacological evaluation of Tic-hydantoin derivatives as selective sigma1 ligands. Part 1. Bioorg Med Chem Lett 15: 4833–4837.

Chhabra S, Chang SC, Nguyen HM, Huq R, Tanner MR, Londono LM *et al.* (2014). Kv1.3 channel-blocking immunomodulatory peptides from parasitic worms: implications for autoimmune diseases. FASEB J 28: 3952–3964.

Cobos EJ, Entrena JM, Nieto FR, Cendán CM, Del Pozo E (2008). Pharmacology and therapeutic potential of sigma(1) receptor ligands. Curr Neuropharmacol 6: 344–366.

Coccini T, Manzo L, Costa LG (1991). 3H-spiperone labels sigma receptors, not dopamine D2 receptors, in rat and human lymphocytes. Immunopharmacology 22: 93–105.

Crespi CL, Miller VP, Penman BW (1997). Microtiter plate assays for inhibition of human, drug-metabolizing cytochromes P450. Anal Biochem 248: 188–190.

Cross AH, O'Mara T, Raine CS (1993). Chronologic localization of myelin-reactive cells in the lesions of relapsing EAE: implications for the study of multiple sclerosis. Neurology 43: 1028–1033.

Dal Canto MC, Melvold RW, Kim BS, Miller SD (1995). Two models of multiple sclerosis: experimental allergic encephalomyelitis (EAE) and Theiler's murine encephalomyelitis virus (TMEV) infection. A pathological and immunological comparison. Microsc Res Tech 32: 215–229.

Demerens C, Stankoff B, Zalc B, Lubetzki C (1999). Eliprodil stimulates CNS myelination: new prospects for multiple sclerosis? Neurology 52: 346–350.

Derocq JM, Bourrié B, Ségui M, Le Fur G, Casellas P (1995). In vivo inhibition of endotoxin-induced pro-inflammatory cytokines production by the sigma ligand SR 31747. J Pharmacol Exp Ther 272: 224–230.

DiLillo DJ, Horikawa M, Tedder TF (2011). B-lymphocyte effector functions in health and disease. Immunol Res 49: 281–292.

El Behi M, Zéphir H, Lefranc D, Dutoit V, Dussart P, Devos P *et al.* (2007). Changes in self-reactive IgG antibody repertoire after treatment of experimental autoimmune encephalomyelitis with anti-allergic drugs. J Neuroimmunol 182: 80–88.

El Behi M, Rostami A, Ciric B (2010). Current views on the roles of Th1 and Th17 cells in experimental autoimmune encephalomyelitis. J Neuroimmune Pharmacol 5: 189–197.

Fletcher JM, Lalor SJ, Sweeney CM, Tubridy N, Mills KH (2010). T cells in multiple sclerosis and experimental autoimmune encephalomyelitis. Clin Exp Immunol 162: 1–11.

Fujino M, Funeshima N, Kitazawa Y, Kimura H, Amemiya H, Suzuki S *et al.* (2003). Amelioration of experimental autoimmune encephalomyelitis in Lewis rats by FTY720 treatment. J Pharmacol Exp Ther 305: 70–77.

Grès MC, Julian B, Bourrié M, Meunier V, Roques C, Berger M *et al.* (1998). Correlation between oral drug absorption in humans, and apparent drug permeability in TC-7 cells, a human epithelial intestinal cell line: comparison with the parental Caco-2 cell line. Pharm Res 15: 726–733.

Hasseldam H, Johansen FF (2010). Neuroprotection without immunomodulation is not sufficient to reduce first relapse severity in experimental autoimmune encephalomyelitis. Neuroimmunomodulation 17: 252–264.

Hedskog L, Pinho CM, Filadi R, Rönnbäck A, Hertwig L, Wiehager B *et al.* (2013). Modulation of the endoplasmic reticulum-mitochondria interface in Alzheimer's disease and related models. Proc Natl Acad Sci U S A 110: 7916–7921.

Iwata Y, Matsushita T, Horikawa M, Dilillo DJ, Yanaba K, Venturi GM *et al.* (2011). Characterization of a rare IL-10-competent B-cell subset in humans that parallels mouse regulatory B10 cells. Blood 117: 530–541.

Kalampokis I, Yoshizaki A, Tedder TF (2013). IL-10-producing regulatory B cells (B10 cells) in autoimmune disease. Arthritis Res Ther 15: S1.

Kilkenny C, Browne W, Cuthill IC, Emerson M, Altman DG (2010). Animal research: Reporting *in vivo* experiments: the ARRIVE guidelines. Br J Pharmacol 160: 1577–1579.

Kourrich S, Su TP, Fujimoto M, Bonci A (2012). The sigma-1 receptor: roles in neuronal plasticity and disease. Trends Neurosci 35: 762–771.

Kozlowski PB, Schuller-Lewis GB, Wisniewski HM (1987). Induction of synchronized relapses in SJL/J mice with chronic relapsing experimental allergic encephalomyelitis. Acta Neuropathol 74: 163–168.

Kuhnz W, Gieschen H (1998). Predicting the oral bioavailability of 19-nortestosterone progestins in vivo from their metabolic stability in human liver microsomal preparations in vitro. Drug Metab Dispos 26: 1120–1127.

Lee-Chang C, Lefranc D, Salleron J, Faveeuw C, Allet C, Vermersch P *et al.* (2011a). Susceptibility to experimental autoimmune encephalomyelitis is associated with altered B-cell subsets distribution and decreased serum BAFF levels. Immunol Lett 135: 108–117.

Lee-Chang C, Top I, Zéphir H, Dubucquoi S, Trauet J, Dussart P *et al.* (2011b). Primed status of transitional B cells associated with their presence in the cerebrospinal fluid in early phases of multiple sclerosis. Clin Immunol 139: 12–20.

Lipinski CA, Lombardo F, Dominy BW, Feeney PJ (2001). Experimental and computational approaches to estimate solubility and permeability in drug discovery and development settings. Adv Drug Deliv Rev 46: 3–26.

Lisak RP, Nedelkoska L, Benjamins JA (2014). Effects of dextromethorphan on glial cell function: proliferation, maturation, and protection from cytotoxic molecules. Glia 62: 751–762.

Magliozzi R, Columba-Cabezas S, Serafini B, Aloisi F (2004). Intracerebral expression of CXCL13 and BAFF is accompanied by formation of lymphoid follicle-like structures in the meninges of mice with relapsing experimental autoimmune encephalomyelitis. J Neuroimmunol 148: 11–123.

Mann MK, Ray A, Basu S, Karp CL, Dittel BN (2012). Pathogenic and regulatory roles for B cells in experimental autoimmune encephalomyelitis. Autoimmunity 45: 388–399.

Mathes C (2006). QPatch: the past, present and future of automated patch clamp. Expert Opin Ther Targets 10: 319–327.

Matsushita T, Yanaba K, Bouaziz JD, Fujimoto M, Tedder TF (2008). Regulatory B cells inhibit EAE initiation in mice while other B cells promote disease progression. J Clin Invest 118: 3420–3430.

Mauri C, Blair PA (2010). Regulatory B cells in autoimmunity: developments and controversies. Nat Rev Rheumatol 6: 636–643.

Mauri C, Bosma A (2012). Immune regulatory function of B cells. Annu Rev Immunol 30: 221–241.

McGrath J, Drummond G, McLachlan E, Kilkenny C, Wainwright C (2010). Guidelines for reporting experiments involving animals: the ARRIVE guidelines. Br J Pharmacol 160: 1573–1576.

Meunier J, Ieni J, Maurice T (2006). Antiamnesic and neuroprotective effects of donepezil against learning impairments induced in mice by exposure to carbon monoxide gas. J Pharmacol Exp Ther 317: 1307–1319.

Miki Y, Mori F, Kon T, Tanji K, Toyoshima Y, Yoshida M *et al.* (2014). Accumulation of the sigma-1 receptor is common to neuronal nuclear inclusions in various neurodegenerative diseases. Neuropathology 34: 148–158.

O'Connor RA, Anderton SM (2008). Foxp3+ regulatory T cells in the control of experimental CNS autoimmune disease. J Neuroimmunol 193: 1–11.

Ono S, Hatanaka T, Hotta H, Satoh T, Gonzalez FJ, Tsutsui M (1996). Specificity of substrate and inhibitor probes for cytochrome P450s: evaluation of in vitro metabolism using cDNA-expressed human P450s and human liver microsomes. Xenobiotica 26: 681–693.

Pawson AJ, Sharman JL, Benson HE, Faccenda E, Alexander SP, Buneman OP *et al.*; NC-IUPHAR (2014). The IUPHAR/BPS Guide to PHARMACOLOGY: an expert-driven knowledge base of drug targets and their ligands. Nucl. Acids Res. 42 (Database Issue): D1098–1106.

Peviani M, Salvaneschi E, Bontempi L, Petese A, Manzo A, Rossi D *et al.* (2014). Neuroprotective effects of the sigma-1 receptor (S1R)

agonist PRE-084, in a mouse model of motor neuron disease not linked to SOD1 mutation. Neurobiol Dis 62: 218–232.

Ransohoff RM (2012). Animal models of multiple sclerosis: the good, the bad and the bottom line. Nat Neurosci 15: 1074–1077.

Sangster J (1997) Octanol-Water Partition Coefficients: Fundamentals and Physical Chemistry, Vol. 2 of Wiley Series in Solution Chemistry. John Wiley & Sons: Chichester.

Stresser DM, Blanchard AP, Turner SD, Erve JC, Dandeneau AA, Miller VP *et al.* (2000). Substrate-dependent modulation of CYP3A4 catalytic activity: analysis of 27 test compounds with four fluorometric substrates. Drug Metab Dispos 28: 1440–1448.

Su TP, Hayashi T, Maurice T, Buch S, Ruoho AE (2010). The sigma-1 receptor chaperone as an inter-organelle signaling modulator. Trends Pharmacol Sci 31: 557–566.

Targoni OS, Baus J, Hofstetter HH, Hesse MD, Karulin AY, Boehm BO *et al.* (2001). Frequencies of neuroantigen-specific T cells in the central nervous system versus the immune periphery during the course of experimental allergic encephalomyelitis. J Immunol 166: 4757–4764.

Toussaint M, Delair B, Foulon C, Lempereur N, Vaccher C, Maurice T *et al.* (2009). Tic hydantoin sigma-1 agonist: pharmacological characterization on cocaine-induced stimulant and appetitive effects. Eur Neuropsychopharmacol 19: 504–515.

Toussaint M, Mousset D, Foulon C, Jacquemard U, Vaccher C, Melnyk P (2010). Sigma-1 ligands: Tic-hydantoin as a key pharmacophore. Eur J Med Chem 45: 256–263.

Tuohy VK, Lu Z, Sobel RA, Laursen RA, Lees MB (1989). Identification of an encephalitogenic determinant of myelin proteolipid protein for SJL mice. J Immunol 142: 1523–1527.

Webb M, Tham CS, Lin FF, Lariosa-Willingham K, Yu N, Hale J *et al.* (2004). Sphingosine 1-phosphate receptor agonists attenuate relapsing-remitting experimental autoimmune encephalitis in SJL mice. J Neuroimmunol 153: 108–121.

Yao H, Duan M, Buch S (2011). Cocaine-mediated induction of platelet-derived growth factor: implication for increased vascular permeability. Blood 117: 2538–2547.

## Supporting information

Additional Supporting Information may be found in the online version of this article at the publisher's web-site:

http://dx.doi.org/10.1111/bph.13037

**Table S1** Effect of σ1 agonist, compound 1(S), on peripheral inflammatory state.